J Appl Physiol
90: 2427–2438, 2001.

Smooth muscle relaxation and local hydraulic impedance properties of the aorta

BERNARD P. CHOLLEY,[1] ROBERTO M. LANG,[1]
CLAUDIA E. KORCARZ,[1] AND SANJEEV G. SHROFF[2]
[1]*Cardiology Section, Department of Medicine, University of Chicago, Chicago, Illinois 60637; and*
[2]*Department of Bioengineering, University of Pittsburgh, Pittsburgh, Pennsylvania 15261*

Received 23 May 2000; accepted in final form 4 January 2001

Cholley, Bernard P., Roberto M. Lang, Claudia E. Korcarz, and Sanjeev G. Shroff. Smooth muscle relaxation and local hydraulic impedance properties of the aorta. *J Appl Physiol* 90: 2427–2438, 2001.—Smooth muscle relaxation is expected to yield beneficial effects on hydraulic impedance properties of large vessels. We investigated the effects of intravenous diltiazem infusion on aortic wall stiffness and local hydraulic impedance properties. In seven anesthetized, closed-chest dogs, instantaneous cross-sectional area and pressure of the descending thoracic aorta were measured using transesophageal echocardiography combined with acoustic quantification and a micromanometer, respectively. Data were acquired during a vena caval balloon inflation, both at the control condition and with diltiazem infusion. At the operating point, diltiazem reduced blood pressure in all dogs but did not alter aortic dimensions or wall stiffness. Over the observed pressure range, aortic area-pressure relationships were linear. Whereas diltiazem affected the slope of this relationship variably (no change in 3 dogs, increase in 1 dog, decrease in 3 dogs), the zero-pressure area intercept was significantly increased in every case such that higher area was observed at any given pressure. When comparisons were made at a common level of wall stress, wall stiffness was either increased or unchanged during diltiazem infusion. In contrast, diltiazem decreased wall stiffness in every case when comparisons were made at a common level of aortic midwall radius. Aortic characteristic impedance and pulse wave velocity, components of left ventricular hydraulic load that are determined by aortic elastic and geometric properties, were affected variably. A comparison of wall stiffness at matched wall stress appears inappropriate for assessing changes in smooth muscle tone. Because of the competing effects of changes in vessel diameter and wall stiffness, smooth muscle relaxation is not necessarily accompanied by the expected beneficial changes in local aortic hydraulic impedance. These results can be reconciled by recognizing that components other than vascular smooth muscle (e.g., elastin, collagen) contribute to aortic wall stiffness.

compliance; incremental elastic modulus; characteristic impedance; pulse wave velocity; calcium channel blocker

AORTIC ELASTIC PROPERTIES play a major role in transforming the pulsatile ejection from the left ventricle (LV) into a continuous flow at the level of the capillaries and in determining the hydraulic load faced by the LV during ejection. These properties are altered with aging (4, 19, 20) or hypertension (4, 17, 21, 26, 44) such that LV afterload is increased, impairing the "ideal" ventriculoarterial coupling (7, 27). Hence, it has been suggested that the pharmacological therapy of hypertension should not only be aimed at reducing elevated systemic vascular resistance but also at improving the decreased distensibility of large arteries (26, 36–39).

Calcium channel blockers are used for the treatment of systemic hypertension. Although it is clear that these agents reduce peripheral vascular resistance (the steady component of hydraulic load imposed by the systemic arterial circulation), some studies have demonstrated that they can also increase large vessel compliance via a reduction in arterial smooth muscle tone (18, 35, 40, 47, 49). Consequently, it is logical to expect that calcium channel blockers will reduce the pulsatile component of systemic arterial hydraulic load as well. However, experimental data have yielded equivocal results. For example, the observation of increased global arterial compliance in hypertensive subjects following acute or chronic administration of calcium channel antagonist nifedipine supports the above-mentioned expectation (10, 12, 45). In contrast, nifedipine administration in these hypertensive subjects did not alter localized measures of pulsatile arterial load, such as aortic characteristic impedance, in a consistent manner; the group-averaged values were unchanged (10, 12, 45). It can be argued, at least on a theoretical basis, that the interplay between changes in distending pressure and vessel geometric and elastic properties underlies this disparity. However, limited in vivo experimental data exist to evaluate this theoretical argument. Until recently, in vivo evaluation of regional aortic geometric and elastic properties was limited due to methodological difficulties encountered in simultaneously acquiring instantaneous measurements of aortic diameter, wall thickness, and pressure. New developments in ultrasound technology, such as transesophageal imaging of the aorta with automated endothelial border detection, have overcome these limita-

Address for reprint requests and other correspondence: S. G. Shroff, Dept. of Bioengineering, Univ. of Pittsburgh, 749 Benedum Hall, Pittsburgh, PA 15261 (E-mail: sshroff@pitt.edu).

The costs of publication of this article were defrayed in part by the payment of page charges. The article must therefore be hereby marked "*advertisement*" in accordance with 18 U.S.C. Section 1734 solely to indicate this fact.

tions by allowing continuous assessment of aortic dimensions (11, 19).

Accordingly, the purpose of this study was to investigate the acute effects of smooth muscle relaxation (as produced by intravenous infusion of diltiazem) on geometric and elastic properties of the aorta. In addition, the consequences of these changes on aortic characteristic impedance and pulse wave velocity, components of LV hydraulic load that are determined by aortic elastic and geometric properties were evealuated. We wished to test the hypothesis that smooth muscle relaxation always yields beneficial changes in localized aortic hydraulic impedance properties (i.e., reduced aortic characteristic impedance and pulse wave velocity).

METHODS

Surgical preparation and data acquisition. Seven mongrel dogs (29 ± 3 kg body wt, male) were studied. All protocols were approved by The University of Chicago Institutional Animal Care and Use Committee and conformed with the National Institutes of Health (NIH) *Guide for the Care and Use of Laboratory Animals* (no. 85–23, revised 1996). Animals received unlimited food and water until 8 h before the study. Anesthesia was induced using intravenous pentobarbital sodium (30 mg/kg) injected via a peripheral vein and maintained throughout the experiment using a constant inspired halothane fraction of 1%. Animals were intubated and mechanically ventilated (respirator model 683, Harvard Apparatus, South Natick, MA) with room air at a frequency of 20 cycles/min. Tidal volume was adjusted to maintain arterial P_{CO_2} between 30 and 40 Torr. Electrocardiogram (ECG) was continuously monitored.

The methodology used for data acquisition has been described previously (11). Briefly, a transesophageal probe (5 MHz, monoplane) connected to an echocardiographic unit (Sonos-1500, Hewlett Packard, Andover, MA) was introduced into the esophagus. The aorta was visualized by rotating the shaft toward the spine of the animal. The transducer was then positioned immediately distal to the off-take of the left subclavian artery, and the aorta was imaged in the transverse plane. Short-axis images of the aorta were optimized by adjusting time- and lateral-gain compensation settings to improve the visualization of the aortic-endothelial interface. The backscatter-based endothelial boundary detection system (31, 32) was then activated, and gain controls were readjusted to enhance the tracking of the aortic endothelium-blood interface. A region of interest was traced around the blood pool cavity. A built-in software package (31, 32) computed and instantaneously displayed aortic lumen area as a function of time (Fig. 1). A data port, providing an electrical analog output of the instantaneous aortic lumen area, was incorporated into the ultrasound imaging system. Without changing the position of the transesophageal transducer, end diastolic aortic diameter and wall thickness were measured from aortic two-dimensional targeted M mode recordings at the time of the R wave on the ECG.

To measure instantaneous aortic pressure, a 6-Fr catheter with a micromanometer at the tip (SPC-360, Millar Instruments, Houston, TX) was introduced retrogradely via a femoral artery and positioned immediately distal to the ultrasonic imaging plane. Instantaneous aortic pressure and area signals were displayed on the monitor of the echo machine (Fig. 1). An 8-Fr balloon-tipped catheter (balloon diameter-40 mm; Medi-tech, Watertown, MA) was positioned in the inferior vena cava (IVC), via a femoral vein, approximately at the level of the diaphragm. Balloon inflation was used to generate a broad range of aortic pressures and areas (11).

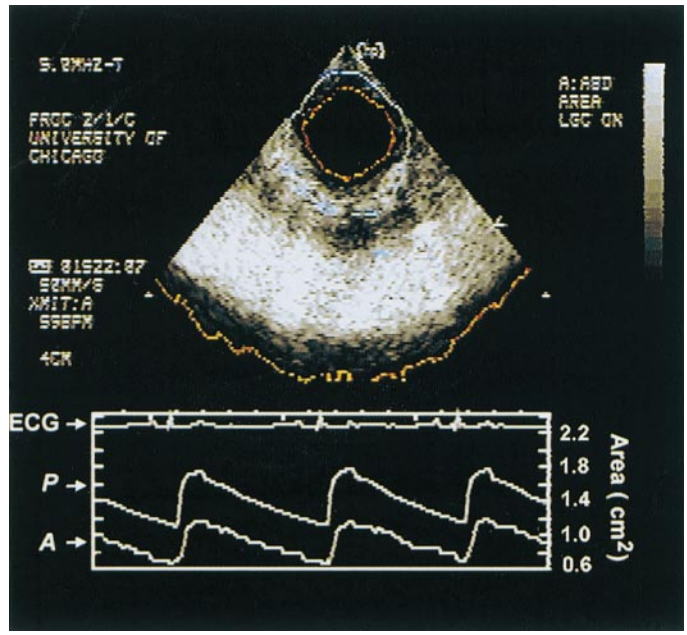

Fig. 1. Two-dimensional image (short-axis view) of the aorta obtained with transesophageal echocardiography (*top*). The aortic endothelium-blood interface (orange line) was identified using an on-line, automated border detection system. Instantaneous aortic lumen cross-sectional area (*A*), aortic pressure (P), and electrocardiogram (ECG) data were recorded simultaneously (*bottom*).

Experimental design. Thirty minutes were allowed for stabilization of the preparation before the initiation of data acquisition. With the respirator turned off, data were acquired during the initial 30 s of IVC balloon inflation. Aortic pressure, aortic area, and ECG data were digitized on-line at 400 Hz and stored on the hard drive of a commercially available computer. After the completion of baseline recordings (control), intravenous diltiazem was injected as a bolus (0.2 mg/kg) followed by a continuous infusion (0.3 $mg \cdot kg^{-1} \cdot h^{-1}$). Data acquisition protocol, similar to the control condition, was repeated 15 min after the initiation of the diltiazem infusion.

Determination of aortic elastic and local hydraulic impedance properties. Two-dimensional imaging of the aorta was performed at a frame rate of 33 Hz. Because the processing delay of the backscatter algorithm approximates the duration of one video frame (46), the digitized aortic area was offset by 30 ms with respect to the pressure recordings. Data acquired during IVC balloon inflation enabled the determination of aortic area-pressure relationships over a wide range of loading conditions. Only peak systolic and minimum diastolic pressures and the corresponding area values from each cardiac cycle during balloon inflation were used to construct the area-pressure relationships. These peak and minimal values correspond to the extremes of the elliptic area-pressure loops where the contribution of the viscous properties may be small (19, 29). Aortic compliance per unit length (C_L) was calculated as the slope of the aortic area-pressure linear regression. Instantaneous aortic thickness was derived from measurements of end-diastolic aortic diameter and wall thickness and then used to compute instantaneous aortic midwall radius and wall stress (see APPENDIX). From the stress-radius relationship, aortic wall stiffness was

quantified in terms of the incremental elastic modulus (E_{inc}) at a given stress or midwall radius (19).

With the use of the pressure, radius, and thickness data, local hydraulic impedance properties were quantified in terms of aortic characteristic impedance (Z_c) and aortic pulse wave velocity (C_{ph}). We calculated Z_c and C_{ph} for any given level of aortic pressure and established the individual Z_c-pressure and C_{ph}-pressure relationships before and after diltiazem infusion. All relevant equations used to compute the derived quantities are presented in the APPENDIX.

Statistical analysis. Data were compared using paired *t*-test (control vs. diltiazem). The Wilcoxon signed rank test was used when the assumption of normal distribution was violated. Least squares regression analysis was performed on area-pressure and stress-midwall radius relationships. The method of excess variance (or extra sum of squares) (34) was used to compare regression parameters between the two conditions (i.e., control vs. diltiazem). A P value <0.05 was considered significant. All results are expressed as means ± SD.

RESULTS

Diltiazem infusion reduced both systolic and diastolic blood pressures in all dogs without significant changes in heart rate (Table 1); pulse pressure increased by a small amount (5 ± 3 mmHg). Despite the fall in blood pressure after infusion of diltiazem, aortic area and change in area during a cardiac cycle (pulse area) at the operating point (i.e., steady-state value just before the IVC balloon inflation) did not change (Table 1).

IVC balloon inflation resulted in a progressive decrease in aortic pressures in all animals, which was accompanied by a reduction in aortic area. Under control conditions, the ranges of aortic pressure and area reductions with IVC balloon inflation were 54 ± 9 mmHg and 0.63 ± 0.18 cm^2, respectively. Similar reductions in pressure and area were noted with IVC balloon inflation during diltiazem infusion (55 ± 13 mmHg and 0.59 ± 0.20 cm^2). All aortic area-pressure relationships were highly linear (median R^2 = 0.961; range-0.830–0.984), and diltiazem shifted these relationships such that aortic area for any pressure was higher during diltiazem infusion in each of the seven dogs (Figs. 2*A* and 3*A*).

Table 1. *Operating point values at control and during diltiazem infusion*

	Control	Diltiazem
HR, beats/min	103 ± 30	100 ± 34
A_S, cm^2	1.52 ± 0.23	1.62 ± 0.45
A_D, cm^2	1.22 ± 0.23	1.23 ± 0.32
Pulse area ($A_S - A_D$), cm^2	0.30 ± 0.11	0.39 ± 0.16
P_S, mmHg	126 ± 22	116 ± 27*
P_D, mmHg	96 ± 13	81 ± 16*
Pulse pressure ($P_S - P_D$), mmHg	30 ± 16	35 ± 19*
C_L, cm^2/mmHg	0.012 ± 0.004	0.011 ± 0.003
σ_S, $\times 10^6$ dyn/cm^2	0.64 ± 0.10	0.63 ± 0.24
σ_D, $\times 10^6$ dyn/cm^2	0.41 ± 0.05	0.35 ± 0.10
E_{inc} at σ_S, $\times 10^6$ dyn/cm^2	2.71 ± 0.79	3.07 ± 1.33
E_{inc} at σ_D, $\times 10^6$ dyn/cm^2	1.56 ± 0.31	1.45 ± 0.46
Z_c at P_S, dyn-s/cm^5	409 ± 76	409 ± 97
Z_c at P_D, dyn-s/cm^5	418 ± 77	405 ± 97
C_{ph} at P_S, cm/s	577 ± 79	595 ± 98
C_{ph} at P_D, cm/s	468 ± 40	449 ± 54

Values are means ± SD (n = 7). HR, heart rate; *A*, aortic lumen cross-sectional area; P, aortic pressure; C_L, aortic compliance per unit length; σ, aortic wall stress; E_{inc}, incremental elastic modulus of the aortic wall; Z_c and C_{ph}, aortic characteristic impedance and pulse wave velocity, respectively. Subscripts S and D denote peak systolic and minimum diastolic values, respectively. *P < 0.05, diltiazem vs. control.

The excess variance analysis indicated that diltiazem infusion did not change the slope of the area-pressure relationship (i.e., C_L) in three dogs (*dogs 1*, *3*, and *4*; Fig. 2*A*); the remaining four dogs had a statistically significant change of +21% in *dog 2* (Fig. 3*A*), −24% in *dog 5*, −39% in *dog 6*, and −16% in *dog 7*. In contrast, the zero-pressure-area intercept was increased significantly in each of the seven dogs (group averages, 0.09 ± 0.27 vs. 0.41 ± 0.24 cm^2). Although the linear extrapolation of the area-pressure relationship to zero pressure may be questionable, these data do indicate that diltiazem infusion shifted the aortic area-pressure relationship leftward over the observed pressure range (i.e., larger area for a given pressure).

Stress-midwall radius relationships were nonlinear (Figs. 2*B* and 3*B*) and fitted well (median R^2 = 0.985; range-0.934–0.994) by an exponential function (see APPENDIX). In response to diltiazem infusion, stress-midwall radius relationships were shifted to the right in all dogs such that, for a given wall stress, midwall radius (Figs. 2*B* and 3*B*) was greater following smooth muscle relaxation. Aortic wall stiffness for a given wall stress was either greater (*dogs 1*, *3*, *5*, *6*, and *7*; Fig. 2*C*) or unchanged (*dogs 2* and *4*; Fig. 2*D*). In contrast, E_{inc} at a given midwall radius was lower during diltiazem infusion in every dog (Figs. 2*D* and 3*D*). At the operating point, however, aortic dimensions and wall stiffness were not different between control and diltiazem (Table 1).

The effects of changes in aortic elastic and geometric properties on local hydraulic impedance properties were quantified in terms of aortic Z_c and C_{ph}. Diltiazem infusion resulted in variable qualitative and quantitative changes in Z_c (Fig. 4); Z_c decreased in 4 dogs (*dogs 1*, *2*, *3*, and *4*) and increased in 2 dogs (*dogs 6* and *7*) over the entire pressure range, whereas it had a mixed effect in the remaining dog (*dog 5*, Z_c-pressure relationships intersected). Despite a beneficial reduction in Z_c in four dogs, none of the dogs exhibited a reduction in C_{ph} following diltiazem (i.e., reduced C_{ph} at a given pressure). In fact, increased C_{ph} at a given pressure was noted in 4 dogs (*dogs 1*, *3*, *5*, and *6*; Fig. 5), whereas the C_{ph}-pressure relationship was unaltered in the remaining three dogs (*dogs 2*, *4*, and *7*; Fig. 5). At the operating point, the mean Z_c and C_{ph} values (i.e., averaged over all 7 dogs) were not different before or after diltiazem (Table 1).

DISCUSSION

In addition to methodological considerations, the following discussion focuses on the two main observations of the study. *1*) Inferences regarding diltiazem-induced

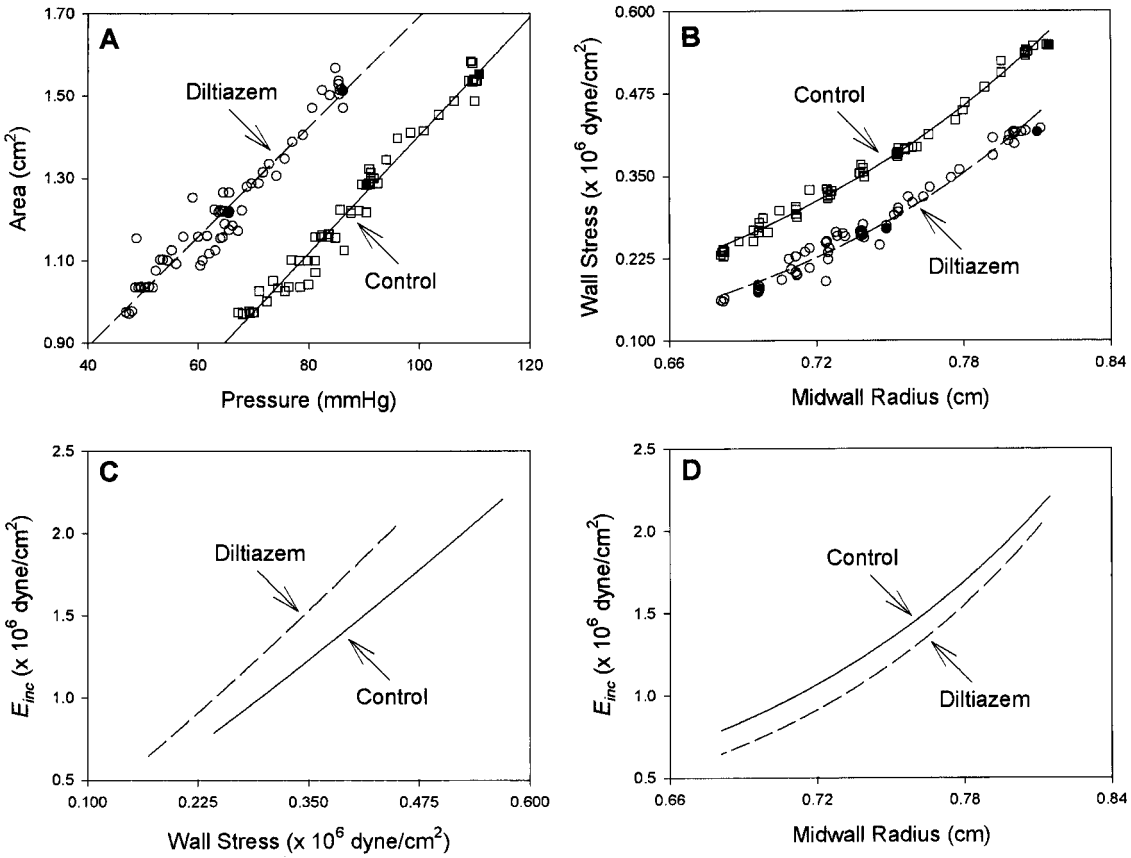

Fig. 2. Aortic lumen area-aortic pressure (*A*) and aortic wall stress-midwall radius (*B*) relationships obtained by inferior vena caval balloon inflation in a single dog (*dog 3*) before (control) and during diltiazem infusion (diltiazem). Solid and dashed lines correspond to the linear (*A*) and exponential (*B*) fit to the measured data (symbols). Solid symbols in *A* and *B* denote the operating point data (i.e., peak systolic and minimum diastolic pressures and corresponding area values just before the onset of balloon inflation). From these data, aortic wall incremental elastic modulus (E_{inc})-aortic wall stress (*C*) and E_{inc}-midwall radius (*D*) relationships were calculated. Although diltiazem shifted the area-pressure relationship such that aortic area for any pressure was higher, the slope of this relationship (i.e., compliance per unit length) was unaffected in this example.

changes in aortic wall stiffness depend on the method of comparison (i.e., common level of wall stress vs. common level of midwall radius). *2*) Smooth muscle relaxation does not necessarily yield the expected beneficial changes in local hydraulic impedance of the aorta in normotensive, anesthetized dogs.

Methodological considerations. The use of transesophageal echocardiography together with the automated border detection to assess regional elastic properties of the descending thoracic aorta has been previously validated in both human and animal studies (11, 19). Before the availability of this technique, instantaneous aortic dimension measurements could only be obtained in opened-chest or chronically instrumented animals using invasive devices such as sonomicrometers or electromechanical calipers. Recently, investigators were able to obtain measurements of aortic diameter or volume without opening the chest using ultrasonic dimension (40, 42) or impedance catheters (16). Transesophageal echocardiography allows measurements of instantaneous lumen area and aortic thickness, variables necessary for the computation of instantaneous aortic wall stress and E_{inc}. Consequently, we were able to obtain in vivo measurements of E_{inc}, a measure of aortic wall stiffness independent of vessel geometry, and to compare aortic elastic properties at matched levels of aortic wall stress or midwall radius.

Although the analog signals for pressure and area were digitized at 400 Hz (or sampling interval of 2.5 ms), the true temporal resolution for the area measurement was limited by the imaging frame rate (33-Hz or 30-ms sampling interval). In other words, the area information for time intervals shorter than 30 ms was generated by interpolating actual measurements obtained at 30-ms intervals (digital-to-analog conversion and low-pass filtering incorporated within the automatic boundary detection system). This would be inadequate for examining aortic properties that critically depend on the temporal synchrony between pressure and area measurements (e.g., viscous and inertial properties). However, the temporal fidelity requirements for quantifying elastic properties are less stringent, especially when one uses only the peak systolic and minimum diastolic pressure points in analysis. Because the rates of area change are small around

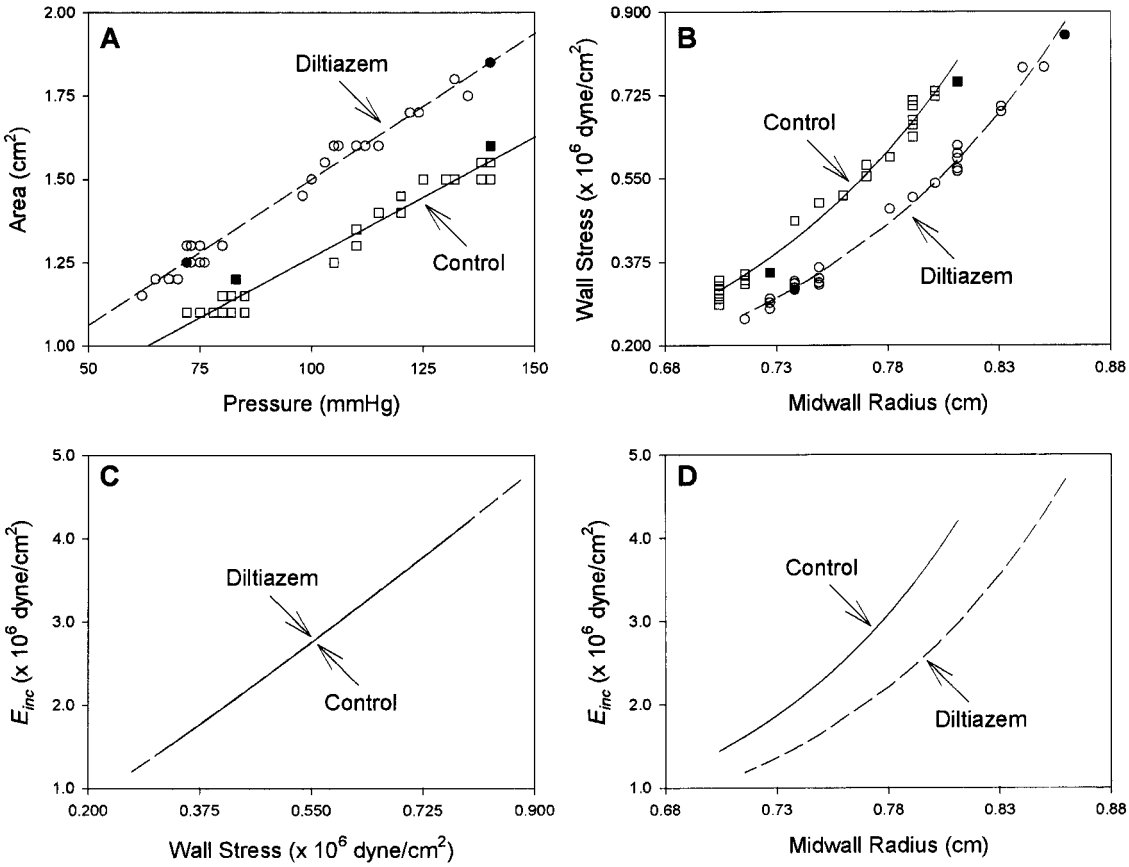

Fig. 3. Aortic lumen area-aortic pressure (*A*) and aortic wall stress-midwall radius (*B*) relationships obtained by inferior vena caval balloon inflation in a single dog (*dog 2*) before (control) and during diltiazem infusion (diltiazem). Aortic wall E_{inc}-wall stress (*C*) and E_{inc}-midwall radius (*D*) relationships were calculated. Similar to the data in Fig. 2, diltiazem shifted the area-pressure relationship such that aortic area for any pressure was higher. However, unlike Fig. 2, the slope of this relationship (i.e., compliance per unit length) was increased.

these points, errors in area measurement due to coarse temporal sampling are expected to be small.

Inflation of a balloon in the IVC was used to construct aortic area-pressure relationships over a wide range of pressures. Nicolosi and Pieper (23, 24) have shown that acute reductions in venous return affect aortic pressure-diameter relationships via reflex changes in sympathetic input to the aorta. The effects on aortic pressure-diameter relationships in their study were measured at 30–45 s after the reduction in venous return. More importantly, these investigators also reported that aortic pressure oscillations with magnitude of ~60 mmHg (a value similar to pressure changes in the present study) and cycle length of 4 s do not invoke reflex responses in anesthetized dogs (23). Thus it appears that the reflex mechanisms do not respond too rapidly. During the first 10–15 s after the onset of balloon inflation in our studies, no increase in heart rate was noted despite a significant drop in aortic pressure. In addition, anesthesia is known to depress smooth muscle responsiveness (1, 28). Taken together, these observations suggest that the sympathetic reflex activation during the initial phase of balloon inflation was probably small. Consequently, the observed alterations in midwall radius, E_{inc}, Z_c, and C_{ph} during balloon inflation most likely reflect the passive changes in regional aortic elastic mechanical properties caused by pressure alterations. Finally, as long as balloon inflation-mediated reflex changes are similar between control and diltiazem conditions, these changes are unlikely to be a confounding factor.

Two pairs of area-pressure data points per cardiac cycle (i.e., peak systolic and minimum diastolic pressures and corresponding area values) were used to generate aortic area-pressure relationships. These discrete points were chosen because they correspond to the extremes of the elliptic area-pressure loop, where the contribution of viscous phenomena may be negligible (19). Thus the area-pressure relationship obtained most likely represents the static elastic behavior of the vessel (29).

The small number of experimental animals (7 dogs) does not negate the main finding of the study that smooth muscle relaxation does not necessarily yield the expected beneficial changes in local hydraulic impedance properties of the aorta; individual animal responses are quite variable. For an individual animal, area and pressure measurements were obtained over a broad range of pressures. These area-pressure relationships (as well as stress-radius relationships) before

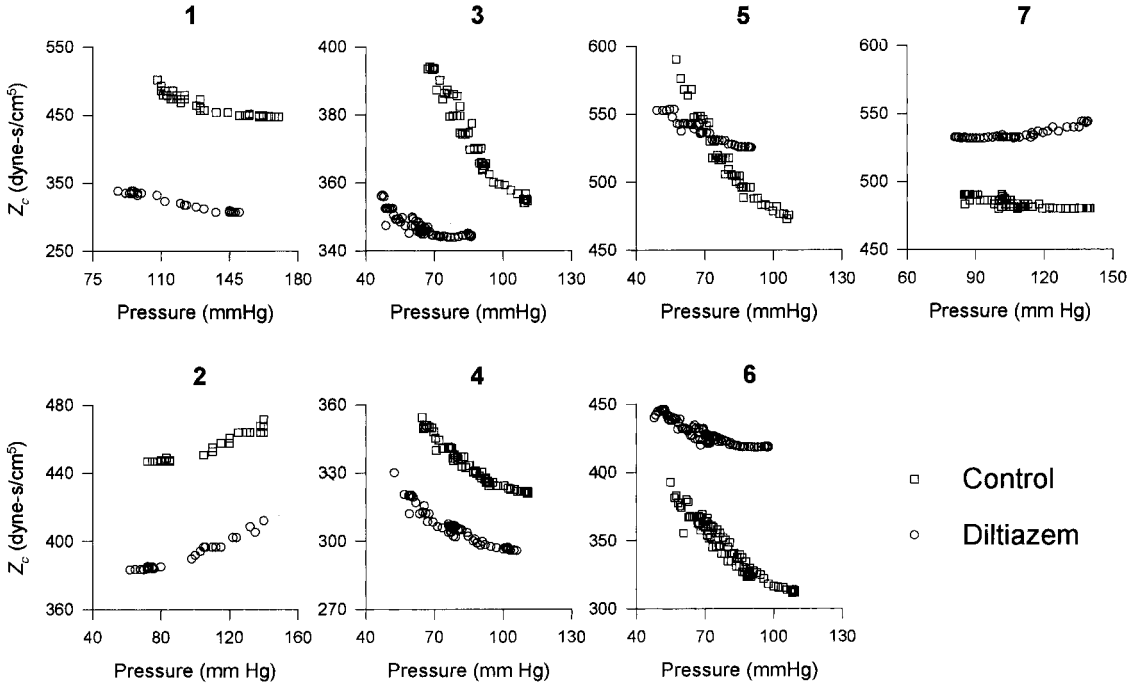

Fig. 4. Individual relationships between aortic characteristic impedance (Z_c) and aortic pressure at control condition and during diltiazem infusion for *dogs 1–7*.

and after smooth muscle relaxation were compared using least square regression analysis and the method of excess variance. Thus the effects of smooth muscle relaxation in an individual animal are supported by appropriate and robust (i.e., with adequate statistical power and significance) statistical testing. It is true that additional experimental animals would have yielded better statistical power for comparing the group-averaged responses (control vs. diltiazem; Table 1). However, this does not have any impact on the statistical validity of individual responses and, consequently, the main finding of this study.

Comparisons of aortic wall elastic properties. When comparisons were made at a common level of wall

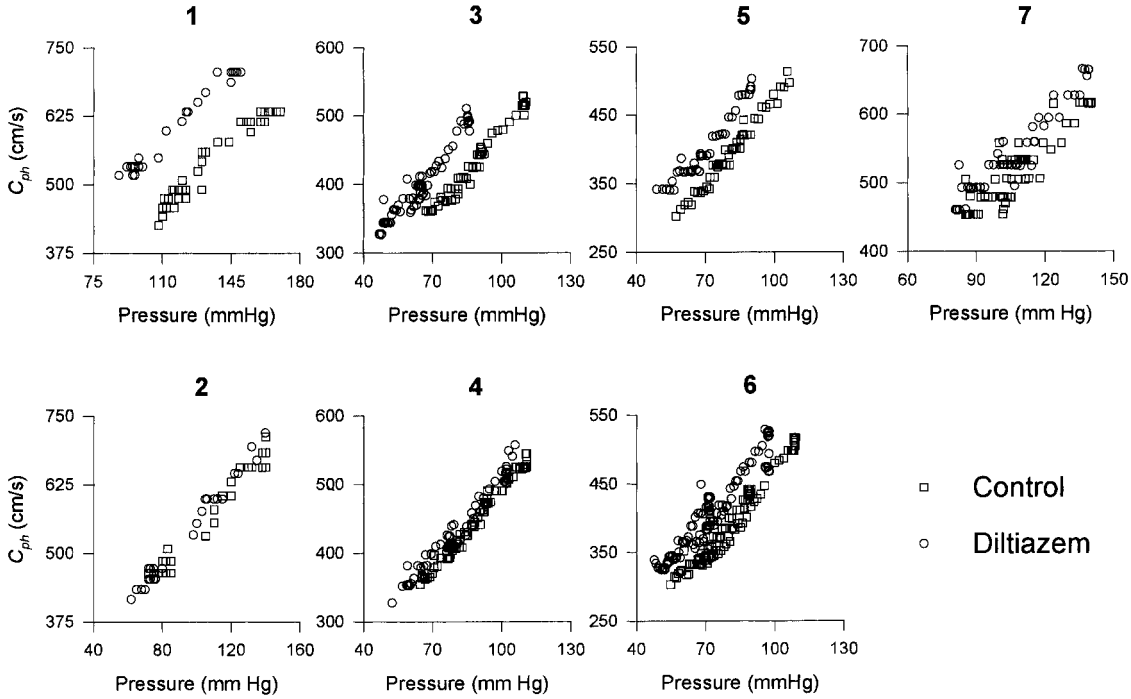

Fig. 5. Individual relationships between aortic pulse wave velocity (C_{ph}) and aortic pressure at control condition and during diltiazem infusion for *dogs 1–7*.

stress, we did not observe a decrease in E_{inc}; in fact, it increased in five of seven dogs. We hypothesize that this "paradoxical" stiffening of the arterial wall during smooth muscle relaxation is due to the stretching/recruiting of passive elastic elements of the aortic wall as the vessel circumference increases (6, 14, 48). In other words, diltiazem-induced smooth muscle relaxation caused redistribution of stress among the various components of aortic wall such that, for a given total wall stress, the stresses borne by elastin and collagen were higher, resulting in a net increase in E_{inc}. This hypothesis is further supported by the result that diltiazem decreased E_{inc} in every case when comparisons were made at a common level of midwall radius (i.e., comparable strain). Thus the observation that diltiazem did not alter aortic dimension and/or wall stiffness at the operating point can be reconciled on the basis of the offsetting effects of reduced distending pressure and reduced smooth muscle tone.

Although changes in E_{inc} are typically compared at a common level of wall stress, comparisons made at common midwall radius were more consistent with the expected changes in the smooth muscle tone. This observation suggests that the comparison of E_{inc} at matched wall stress is inappropriate for assessing changes in smooth muscle tone. This conclusion is in agreement with earlier observations of Dobrin and Rovick (14) and Barra et al. (6).

Aortic area-pressure relationships. The dose of diltiazem used in this study is comparable to that used in humans. This dose produced an average of 13% reduction in mean blood pressure (106 ± 15 to 92 ± 18 mmHg; $P = 0.01$) without inducing a simultaneous change in aortic cross-sectional area. The drop in distending pressure was expected to reduce passively aortic short-axis area, but this was not observed because the "active" drug-induced relaxation of aortic smooth muscle tone counterbalanced this effect. Other investigators conducting comparable studies noted either no change (18, 47) or a decrease (47, 49) in aortic dimensions following infusion of a calcium channel blocker. These differences underscore the variable balance occurring between the active and passive phenomena in different experimental protocols.

We observed highly linear aortic area-pressure relationships, both under control conditions and during diltiazem infusion, implying that C_L was constant over the range of pressure studied. These findings are consistent with some of the previous reports (5, 33). However, other investigators, using aortic constriction to produce very high pressures, were able to demonstrate nonlinearities in aortic pressure-diameter relationships (3, 18, 49).

Although diltiazem increased aortic area at any given pressure in all dogs, no significant changes in local compliance (i.e., slope of the area-pressure relationship) were noted. The two independent determinants of C_L are vessel geometry [mostly diameter because length is relatively fixed (30)] and wall stiffness. With diltiazem, neither the aortic short-axis area nor incremental elastic modulus was altered significantly at the operating point, and, consequently, compliance per unit length was unchanged. However, the leftward shift of the area-pressure relationship [i.e., a larger area at a common level of pressure (Figs. 2*A* and 3*A*)] clearly indicates a physical alteration in the vessel mechanical characteristics following diltiazem administration.

In anesthetized dogs, two studies using comparable doses of diltiazem reported increases in local compliance of the thoracic aorta as quantified by the ratio of the change in lumen diameter to the change in pressure (47, 49). However, these diltiazem-induced changes were quite small (~5%) and therefore do not contradict the present observations. In contrast, diltiazem significantly increased (~50%) the aortic distensibility index in awake normotensive and hypertensive humans (40). For the sake of comparison, we computed the same distensibility index (*Eq. 10* in APPENDIX) from our data and found no difference before or after diltiazem at operating points (0.0044 ± 0.0013 vs. 0.0047 ± 0.0017 $mmHg^{-1}$, respectively). Anesthesia is known to depress the smooth muscle responsiveness (1, 28); this may account for the difference observed between anesthetized animals and awake humans. Furthermore, we examined the effects of smooth muscle relaxation at a single dose of diltiazem. The variability of responses in local hydraulic impedance properties may be less at other (higher) doses. Therefore, our data should not be interpreted to imply anything about the clinical efficacy of diltiazem; clearly, this evaluation would depend on the experimental conditions (e.g., drug dose, anesthetized vs. awake state, normotension vs. hypertension, normal vs. diseased vessels). Other pharmacological treatments [e.g., angiotensin I-converting enzyme (ACE) inhibitors or ACE inhibitors in combination with calcium antagonists] have been found to have beneficial effects on aortic elastic and local hydraulic impedance properties in hypertensive patients (8, 9). Similarly, nifedipine, a calcium channel antagonist, has been reported to significantly increase the distensibility index in both the ascending aorta of human subjects (41) and the descending thoracic aorta of dogs (18). Thus our results with diltiazem should not be taken as representative of other vasodilators that affect smooth muscle by different mechanisms. Instead, we wish to focus on the message that smooth muscle relaxation does not necessarily yield the desired reduction in wall stiffness and local hydraulic impedance (i.e., simultaneous decrease in Z_c and C_{ph}) and discuss the reasons for this observation.

Relationship to systemic arterial hydraulic load. From the perspective of the LV and mechanical function of the coupled LV-arterial system, only alterations in hydraulic load are relevant. LV hydraulic load consists of two components: *1*) a steady component, determined by arteriolar properties and quantified by the systemic vascular resistance (SVR), and *2*) a pulsatile component, mostly determined by the vascular viscoelastic properties and the distributed vascular architecture that gives rise to wave propagation and reflections. Our laboratory (12) and other workers (10, 45)

have shown that nifedipine reduces SVR. Thus it is likely that diltiazem reduces SVR as well, although we did not experimentally evaluate this component of LV load in the present study (cardiac output was not measured). Changes in the regional aortic elastic and geometric properties determine two aspects of the pulsatile component of LV hydraulic load: Z_c, which represents the hydraulic load due to the aorta itself and plays an important role in determining the pulsatility of aortic pressure and flow, and C_{ph}, which is important in determining the characteristics of pressure- and flow-wave propagation and reflections. Reductions in Z_c and C_{ph} would lower LV hydraulic load and are considered to be beneficial changes. Although both Z_c and C_{ph} are equally sensitive to changes in wall stiffness ($\propto E_{inc}^{1/2}$), their respective sensitivities to geometric properties [e.g., internal radius (R_i)] are quite different (*Eqs. 8* and *9* in APPENDIX): $Z_c \propto\sim R_i^{-5/2}$ and $C_{ph} \propto\sim R_i^{-1/2}$. Therefore, according to the relative changes in R_i and E_{inc} following the diltiazem-induced pressure drop in each animal, Z_c and C_{ph} for a given aortic pressure could either decrease, increase, or remain unchanged. Over comparable ranges of pressure, our Z_c-pressure relationships are similar to those described by Stone and Dujardin (43). These authors found that smooth muscle activation elicited by hemorrhage consistently resulted in increased Z_c at matched distending pressure, mainly as a consequence of aortic diameter reduction and some degree of wall stiffening (15, 43). Unlike hemorrhage, wherein both geometric and elastic properties change so as to increase Z_c (reduced radius and increased E_{inc}), diltiazem-induced changes had competing effects on Z_c (increased radius and E_{inc} for a given pressure). This resulted in the variability of the absolute magnitude of Z_c response. On the basis of the leftward shift of the area-pressure relationship, it is clear that diltiazem induced smooth muscle relaxation in every dog. However, this smooth muscle relaxation caused the expected reduction in Z_c in only four of seven dogs, and the expected reduction in C_{ph} was never observed (Fig. 5). In fact, four of seven dogs had increased C_{ph} following diltiazem infusion. Thus diltiazem-induced smooth muscle relaxation does not necessarily yield the expected beneficial effects on local hydraulic impedance in anesthetized dogs with normal vessels.

Components other than vascular smooth muscle (e.g., elastin, collagen) contribute to aortic wall stiffness. Collagen is significantly stiffer than the other two components, and its relative contribution increases with increments in aortic radius (strain). Thus the smooth muscle relaxation-induced decrease in wall stiffness may be offset by the increased contribution of collagen that is associated with increased radius. A theoretical analysis was performed to further explore this possibility. A mathematical model of aortic elastic behavior was formulated (see APPENDIX for details). Smooth muscle relaxation was simulated by reducing the relative smooth muscle tone from 0.50 (control condition) to 0.34; other parameter values were unchanged (APPENDIX). Results of these simulations are presented in Fig. 6. Over the experimentally observed ranges of aortic pressure (demarcated by the solid symbols in Fig. 6), simulated smooth muscle relaxation affected area-pressure (Fig. 6*A* vs. Fig. 2*A*), wall stress-midwall radius (Fig. 6*B* vs. Fig. 2*B*), E_{inc}-wall stress (Fig. 6*C* vs. Fig. 2*C*), E_{inc}-midwall radius (Fig. 6*D* vs. Fig. 2*D*), Z_c-pressure (Fig. 6*E* vs. Fig. 4, *dog 3*), and C_{ph}-pressure (Fig. 6*F* vs. Fig. 5, *dog 3*) relationships in a manner identical to the effects of diltiazem observed in the experiment. Significant nonlinearity in the area-pressure relationship was observed in the simulation study; however, this occurred at pressures greater than 130 mmHg. Certain differences between experimental and simulation results were noted [e.g., more pronounced nonlinearity and minima for Z_c-pressure relationships in the simulation study (Fig. 6*E* vs. Fig. 4, *dog 3*) and nonlinear E_{inc}-wall stress relationships in the simulation study (Fig. 6*C* vs. Fig. 2*C*)]. Despite these differences, simulation results clearly support the main observation of the present study: smooth muscle relaxation does not necessarily yield the expected beneficial changes in local hydraulic impedance of the aorta. After a reduction in smooth muscle tone, wall stress and E_{inc} at a common level of pressure (100 mmHg) increased by 12.4 and 57.3%, respectively. The relative contributions of collagen to wall stress and E_{inc} increased as well [from 0.2% (control) to 1.4% ($\downarrow$ tone) for wall stress and from 2.9% (control) to 15.0% (reduced tone) for E_{inc}]. Thus simulation-based results clearly demonstrate that a reduction in smooth muscle tone can alter relative contributions of vessel wall components; this redistribution can explain our experimental observations.

Although results of the simulation study are consistent with our experimental data, they do not identify specific reasons for the observed interanimal variability of responses. Although all dogs were male and normotensive, there could have been differences in age and life history, leading to interanimal differences in vessel wall composition, smooth muscle tone under control condition, and the extent of smooth muscle relaxation. Because no independent measurements of these factors were made in the present study, we cannot examine the determinants of the interanimal variability of responses. Further studies are necessary to address this important issue.

We have evaluated impedance properties at a single location in the cardiovascular system (i.e., at the point of pressure and area measurements in the descending thoracic aorta). Clearly, other parts of the systemic arterial circulation contribute to the overall pulsatile load as seen by the LV. Because vessel wall composition (especially, the smooth muscle content) and geometric properties vary, other parts of the arterial circulation may respond to smooth muscle relaxation differently from that observed for the aorta. This, in part, may explain our previous observations regarding the disparity in responses of global arterial compliance (AC) and Z_c to vasoactive drugs: both nifedipine and ramipril (ACE inhibitor) consistently increased AC in hypertensive subjects but left Z_c unaffected (12). In

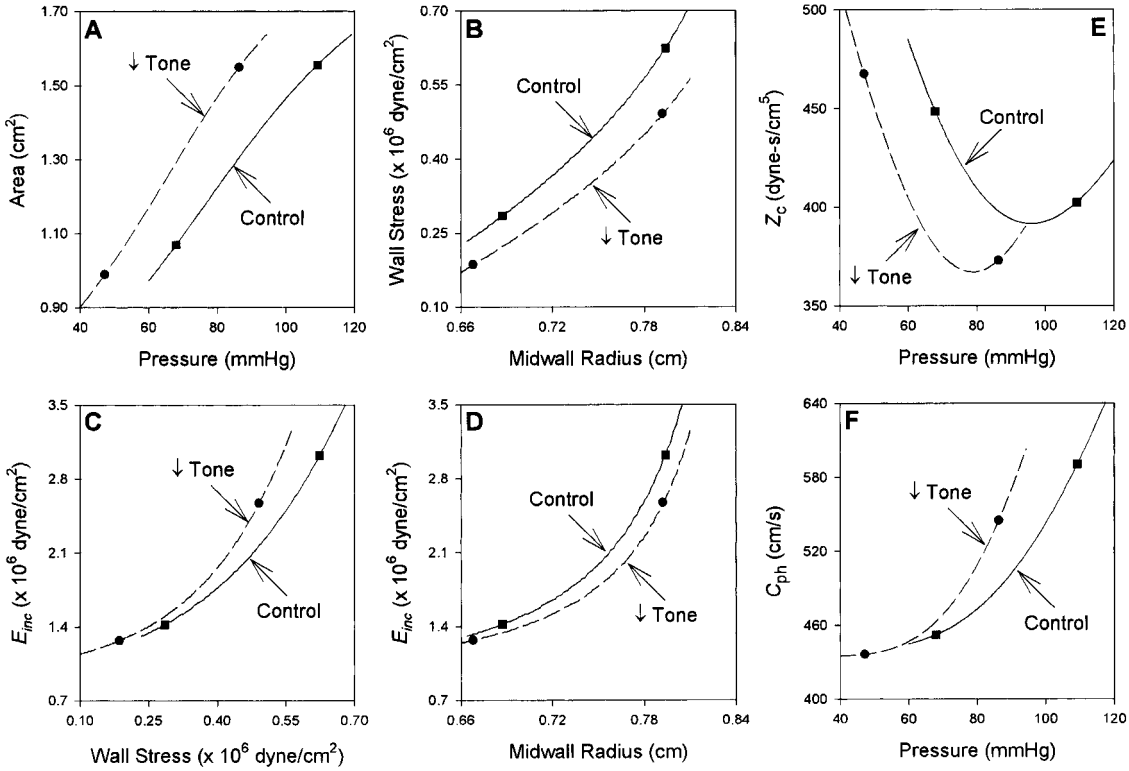

Fig. 6. Results from a mathematical simulation study. Reduced smooth muscle tone (↓ Tone) was simulated by altering the tone parameter; all other parameters were held constant at control values (see APPENDIX). The responses following a reduction of smooth muscle tone are identical to those seen following diltiazem infusion in 1 of the experiments (*dog 3*): Compare *A–D* with Fig. 2, *E* with Fig. 4 (*dog 3*), and *F* with Fig. 5 (*dog 3*). Solid symbols demarcate the pressure ranges over which data were collected from the 2 experimental conditions (■, control; ●, diltiazem) (*dog 3*).

agreement with the AC response, both the first and the second harmonic of the input impedance spectrum were reduced with nifedipine or ramipril (12). Whereas Z_c is determined exclusively by the localized aortic geometric and wall elastic properties, AC is determined by the entire systemic circulation. Although it would be useful to examine the responses to smooth muscle relaxation of vessels other than the aorta, our data are still relevant to the main message of the study that smooth muscle relaxation does not necessarily yield the desired reduction in wall stiffness and local hydraulic impedance (i.e., simultaneous decreases in Z_c and C_{ph}).

A direct extrapolation of our observations derived from normotensive animals with normal vessels to hypertensive animals with remodeled vessels may be questionable. The responses in the latter case would depend on the baseline smooth muscle tone and the interplay among changes in smooth muscle tone, distending pressure, and vessel elastic and geometric properties. It is encouraging, however, to note that nifedipine did not reduce aortic Z_c in hypertensive human subjects (10, 12, 45), a result consistent with our present observations.

Acute reduction of smooth muscle tone after intravenous administration of diltiazem in anesthetized, normotensive dogs shifts the aortic area-pressure relationship leftward without a significant change in aortic distensibility (C_L). Inferences regarding the effects of diltiazem on aortic wall stiffness depend on whether the comparisons are made at matched wall stress (increased or unchanged stiffness) or matched midwall radius (decreased stiffness). Our data support the notion that a comparison of wall stiffness at matched wall stress is inappropriate for assessing changes in smooth muscle tone. Finally, diltiazem affects the aortic contribution to LV hydraulic load (i.e., Z_c and C_{ph}) in a variable manner because of the competing effects of changes in vessel diameter and wall stiffness. This underscores the difficulty in predicting the in vivo effects of a vasoactive agent on large vessel hydraulic impedance properties based solely on the knowledge of its in vitro smooth muscle relaxation properties.

APPENDIX

Calculations of Aortic Wall Stress and Local Hydraulic Impedance Properties

Measurements of end-diastolic aortic diameter (D) and wall thickness (h) were used to calculate the "muscle" area (A_m) surrounding the vessel lumen using the following formula

$$A_m = \pi \times \left(\frac{D}{2} + h\right)^2 - \pi \times \left(\frac{D}{2}\right)^2 = \pi \times h \times (D + h) \quad (1)$$

Assuming an incompressible aortic wall and negligible longitudinal shortening (i.e., constant A_m throughout the cardiac cycle), instantaneous aortic wall thickness [$h(t)$] was calculated from measured instantaneous aortic lumen area [$A(t)$] as

$$h(t) = \sqrt{\frac{A_m + A(t)}{\pi}} - \sqrt{\frac{A(t)}{\pi}} \quad (2)$$

Instantaneous aortic internal [$R_i(t)$], external [$R_o(t)$], and midwall [$R_m(t)$] radii were computed as

$$R_i(t) = \sqrt{\frac{A(t)}{\pi}} \quad (3)$$

$$R_o(t) = \sqrt{\frac{A_m + A(t)}{\pi}} \quad (4)$$

$$R_m(t) = \frac{R_i(t) + R_o(t)}{2} \quad (5)$$

Instantaneous aortic wall stress [$\sigma(t)$] was calculated from measured instantaneous aortic pressure [$P(t)$] using the following formula (28)

$$\sigma(t) = 2P(t) \times \left[\frac{R_i(t) \times R_o(t)}{R_m(t)}\right]^2 \times [R_o^2(t) - R_i^2(t)]^{-1} \quad (6)$$

After the σ-R_m relationship was fitted by an exponential function ($\sigma = \alpha e^{\beta R_m}$, where α and β are constants), E_{inc} for a given σ was calculated as (28)

$$E_{inc}(\sigma) = 0.75 \times R_m \times d\sigma/dR_m \quad (7)$$

Z_c and C_{ph} were calculated according to the following formulas (ρ: blood density) (22, 25)

$$Z_c = \sqrt{\frac{\rho}{3\pi^2}\frac{E_{inc}h(2R_i + h)}{R_i^4(R_i + h)^2}} \quad (8)$$

$$C_{ph} = \sqrt{\frac{1}{3\rho}\frac{E_{inc}h(2R_i + h)}{(R_i + h)^2}} \quad (9)$$

Aortic distensibility index was calculated as

$$\frac{\frac{D_S}{D_D} - 1}{P_S - P_D} = \frac{\sqrt{\frac{A_S}{A_D}} - 1}{P_S - P_D} \quad (10)$$

where subscripts S and D refer to maximum systolic and minimum diastolic values, respectively.

Mathematical Model of Aortic Elastic Behavior

The model formulation is based on the conceptual framework originally proposed by Cox (13) and subsequently extended by Armentano and colleagues (2, 3, 6) to include the smooth muscle component. Briefly, aortic wall was represented as a parallel combination of three compartments (elastin, collagen, and smooth muscle), each having a specified σ-strain (ϵ) relationship (subscripts e, c, and sm denote elastin, collagen, and smooth muscle, respectively). A linear σ-ϵ relationship was assumed for elastin

$$\sigma_e = a_1(\epsilon - a_2) \quad (11)$$

$$E_{inc,e} = \frac{d\sigma_e}{d\epsilon} = a_1 \quad (12)$$

where $E_{inc,e}$ is the incremental elastic modulus of elastin, and a_1 and a_2 are parameters. The elastic behavior of collagen was simulated using the concept of strain-dependent recruitment of collagen (2, 3, 13). A sigmoidally shaped recruitment function (f_r) was used, which varied from a value of 0 at low strains to a value of 1 at high strains (*Eq. 13*). The incremental elastic modulus of collagen ($E_{inc,c}$) was modulated by f_r, such that it asymptotically rose to a maximum value at high strains (parameter a_5 in *Eq. 14*).

$$f_r = \frac{1}{1 + \exp[-a_3(\epsilon - a_4)]} \quad (13)$$

$$E_{inc,c} = \frac{d\sigma_c}{d\epsilon} = a_5 f_r \quad (14)$$

$$\sigma_c = \int_0^{\epsilon} E_{inc,c}\, d\epsilon = \frac{a_5}{a_3}\log\left\{\left(\frac{1 + \exp[-a_3(\epsilon - a_4)]}{\exp[-a_3(\epsilon - a_4)]}\right)\left(\frac{\exp[a_3 a_4]}{1 + \exp[a_3 a_4]}\right)\right\} \quad (15)$$

where a_3–a_5 are parameters. The elastic behavior of smooth muscle was simulated using a strain-dependent activation function, f_a (2). A modified Lorentzian function was used to represent f_a, which is a skewed unimodal function of strain (2)

$$f_a = \frac{a_6\epsilon + a_7}{a_8 + a_9(\epsilon - a_{10})^2} \quad (16)$$

$$\frac{df_a}{d\epsilon} = \frac{a_6 a_8 + a_6 a_9(\epsilon - a_{10})^2 - 2a_9(a_6\epsilon + a_7)(\epsilon - a_{10})}{[a_8 + a_9(\epsilon - a_{10})^2]^2} \quad (17)$$

$$\sigma_{sm} = T_{sm}(a_{11} f_a \epsilon) \quad (18)$$

$$E_{inc,sm} = \frac{d\sigma_{sm}}{d\epsilon} = T_{sm}\left[a_{11}\left(f_a + \epsilon\frac{df_a}{d\epsilon}\right)\right] \quad (19)$$

where $E_{inc,sm}$ is the incremental elastic modulus of smooth muscle, a_6–a_{11} are parameters, and T_{sm} is the user-specified value of relative smooth muscle tone (range: 0 to 1).

For given values of smooth muscle tone and parameters a_1–a_{11}, one can calculate the three stresses (σ_e, σ_c, σ_{sm}; *Eqs. 11*, *15*, and *18*) and three incremental elastic moduli ($E_{inc,e}$, $E_{inc,c}$, $E_{inc,sm}$; *Eqs. 12*, *14*, and *19*) corresponding to any strain. σ and E_{inc} were calculated using the three individual component values and the relative amounts of elastin (W_e), collagen (W_c), and smooth muscle (W_{sm}) in the aortic wall

$$\sigma = W_e\sigma_e + W_c\sigma_c + W_{sm}\sigma_{sm} \quad (20)$$

$$E_{inc} = W_e E_{inc,e} + W_c E_{inc,c} + W_{sm} E_{inc,sm} \quad (21)$$

Given values of unstressed midwall radius (R_{mo}) and cross-sectional A_m, R_m, R_i, and R_o for any strain were calculated as

$$R_m = R_{mo}\epsilon \quad (22)$$

$$R_i = R_m - \frac{A_m}{4\pi R_m} \quad (23)$$

$$R_o = R_m + \frac{A_m}{4\pi R_m} \quad (24)$$

Once σ, E_{inc}, R_m, R_i, and R_o were known for a given strain, aortic P, Z_c, and C_{ph} were calculated using *Eqs. 6*, *8*, and *9*, respectively. The following parameter values were used for the simulation: $a_1 = 2.7 \times 10^6$ dyn/cm^2, $a_2 = 0.9$, $a_3 = 30$, $a_4 = 1.4$, $a_5 = 1.0 \times 10^9$ dyn/cm^2, $a_6 = -71.23$, $a_7 = 93.45$, $a_8 = -0.49$, $a_9 = 997.98$, $a_{10} = 1.337$, $a_{11} = 4.0 \times 10^6$

dyn/cm^2; $W_e = 0.31$, $W_c = 0.21$, W_{sm}, $= 0.48$, $R_{mo} = 0.682$ cm, and $A_m = 0.9$ cm^2. These values were chosen based on the present data and published information (2, 3, 6, 13, 22) with some modifications to fit our control data for *dog 3*. To simulate smooth muscle relaxation, only the relative smooth muscle tone was reduced (smooth muscle tone = 0.5 for control, and 0.34 for reduced tone); all other parameters were held constant.

We thank Dr. Theodore Karrison for his help with the statistical analysis and associated discussion.

This study was supported in part by National Institute on Aging Grant R01-AG-13920 to S. G. Shroff and a French Ministère des Affaires Etrangères (Fondation Lavoisier) grant to B. P. Cholley.

Present address of B. P. Cholley: Anesthesiology and Intensive Care Dept., Hôpital Lariboisière, Paris, France.

REFERENCES

1. **Altura BT and Altura BM.** Pentobarbital and contraction of vascular smooth muscle. *Am J Physiol* 229: 1635–1640, 1975.
2. **Armentano RL, Barra JG, Levenson J, Simon A, and Pichel RH.** Arterial wall mechanics in conscious dogs: assessment of viscous, inertial, and elastic moduli to characterize aortic wall behavior. *Circ Res* 76: 468–478, 1995.
3. **Armentano RL, Levenson J, Barra JG, Fischer SIC, Breitbart GJ, Pichel RH, and Simon AC.** Assessment of elastin and collagen contribution to aortic elasticity in conscious dogs. *Am J Physiol Heart Circ Physiol* 260: H1870–H1877, 1991.
4. **Bader H.** Importance of gerontology of elastic arteries in the development of essential hypertension. *Clin Physiol Biochem* 1: 36–56, 1983.
5. **Barnett GO, Mallos AJ, and Shapiro A.** Relationship of aortic pressure and diameter in the dog. *J Appl Physiol* 16: 545–548, 1961.
6. **Barra JG, Armentano RL, Levenson J, Fischer EIC, Pichel RH, and Simon AC.** Assessment of smooth muscle contribution to descending thoracic aortic elastic mechanics in conscious dogs. *Circ Res* 73: 1040–1050, 1993.
7. **Belz GG.** Elastic properties and Windkessel function of the human aorta. *Cardiovasc Drugs Ther* 9: 73–83, 1995.
8. **Breithaupt-Grogler K, Gerhardt G, Lehmann G, Notter T, and Belz GG.** Blood pressure and aortic elastic properties—verapamil SR/trandolapril compared with a metoprolol/hydrochlorothiazide combination therapy. *Int J Clin Pharmacol Ther* 36: 425–431, 1998.
9. **Breithaupt-Grogler K, Leschinger M, Belz GG, Butzer R, Erb K, de Mey C, and Sinn W.** Influence of antihypertensive therapy with cilazapril and hydrochlorothiazide on stiffness of the aorta. *Cardiovasc Drugs Ther* 10: 49–57, 1996.
10. **Chang KC, Hsieh KS, Kuo TS, and Chen HI.** Effects of nifedipine on systemic hydraulic vascular load in patients with hypertension. *Cardiovasc Res* 24: 719–726, 1990.
11. **Cholley BP, Shroff SG, Korcarz C, and Lang RM.** Aortic elastic properties using transesophageal echocardiography with automated border detection: validation according to regional differences between proximal and distal descending thoracic aorta. *J Am Soc Echocardiogr* 9: 539–548, 1996.
12. **Cholley BP, Shroff SG, Sandelski J, Korcarz C, Balasia BA, Jain S, Berger DS, Murphy MB, Marcus RH, and Lang RM.** Differential effects of chronic oral antihypertensive therapies on systemic arterial circulation and ventricular energetics in African-American patients. *Circulation* 91: 1052–1062, 1995.
13. **Cox RH.** Passive mechanics and connective tissue composition of canine arteries. *Am J Physiol Heart Circ Physiol* 234: H533–H541, 1978.
14. **Dobrin PB and Rovick AA.** Influence of vascular smooth muscle on contractile mechanics and elasticity of arteries. *Am J Physiol* 217: 1644–1651, 1969.
15. **Dujardin JPL, Stone DN, Paul LT, and Pieper HP.** Response of systemic arterial input impedance in volume expansion and hemorrhage. *Am J Physiol Heart Circ Physiol* 238: H902–H908, 1980.
16. **Ferguson JJ, Miller MJ, Sahagian P, Aroesty JM, and McKay RG.** Assessment of aortic pressure-volume relationships with an impedance catheter. *Cathet Cardiovasc Diagn* 15: 27–36, 1988.
17. **Isnard RN, Pannier BM, Laurent S, London GM, Diebold B, and Safar ME.** Pulsatile diameter and elastic modulus of the aortic arch in essential hypertension: a noninvasive study. *J Am Coll Cardiol* 13: 399–405, 1989.
18. **Kohno M, Kumada T, Ozaki M, Matsuzaki M, Katayama K, Fujii T, Miura T, Kohtoki S, Yatabe S, Yano M, Hiro T, and Kusukawa R.** Evaluation of aortic wall distensibility by aortic pressure-dimension relation: effects of nifedipine on aortic wall. *Cardiovasc Res* 21: 305–312, 1987.
19. **Lang RM, Cholley BP, Korcarz C, Marcus RH, and Shroff SG.** Measurements of regional elastic properties of the human aorta: a new application of transesophageal echocardiography with automated border detection and calibrated subclavian pulse tracings. *Circulation* 90: 1875–1882, 1994.
20. **Learoyd BM and Taylor MG.** Alterations with age in the viscoelastic properties of human arterial walls. *Circ Res* 18: 278–292, 1966.
21. **Liu Z, Ting CT, Zhu S, and Yin FCP.** Aortic compliance in human hypertension. *Hypertension* 14: 129–136, 1989.
22. **Milnor WR.** *Hemodynamics.* Baltimore, MD: Williams and Wilkins, 1989.
23. **Nicolosi GR and Pieper HP.** Aortic smooth muscle responses to changes in venous return studied in intact dogs. *Am J Physiol* 221: 1209–1216, 1971.
24. **Nicolosi GR and Pieper HP.** Nature of aortic smooth muscle responses to changes in venous return in intact dogs. *Am J Physiol* 228: 518–525, 1975.
25. **Noordergraaf A.** *Circulatory System Dynamics*. New York: Academic, 1978.
26. **O'Rourke MF.** Arterial stiffness, systolic blood pressure, and logical treatment of arterial hypertension. *Hypertension* 15: 339–347, 1990.
27. **O'Rourke MF, Avolio AP, and Nichols WW.** Left ventricular-systemic arterial coupling in humans and strategies to improve coupling in disease states. In: *Ventricular/Vascular Coupling*: *Clinical, Physiological, and Engineering Aspects,* edited by Yin FCP. New York: Springer Verlag, 1986, p. 1–19.
28. **Pagani M, Mirsky I, Baig H, Thomas MW, Kerkhof P, and Vatner SF.** Effects of age on aortic pressure-diameter and elastic stiffness-stress relationships in unanesthetized sheep. *Circ Res* 44: 420–429, 1979.
29. **Patel DJ, De Freitas FM, Greenfield JC, and Fry DL.** Relationship of radius to pressure along the aorta in living dogs. *J Appl Physiol* 18: 1111–1117, 1963.
30. **Patel DJ and Fry DL.** In situ pressure-radius-length measurements in ascending aorta of anesthetized dogs. *J Appl Physiol* 19: 413–416, 1964.
31. **Perez JE, Klein SC, Prater DM, Fraser CE, Cardona H, Waggoner AD, Holland MR, Miller JG, and Sobel BE.** Automated on-line quantification of left ventricular dimensions and function by echocardiography with backscatter imaging and lateral gain compensation. *Am J Cardiol* 70: 1200–1205, 1992.
32. **Perez JE, Waggoner AD, Barzilai B, Melton HE, Miller JG, and Sobel BE.** On-line assessment of ventricular function by automatic boundary detection and ultrasonic backscatter imaging. *J Am Coll Cardiol* 19: 313–320, 1992.
33. **Pieper HP and Paul LT.** Responses of aortic smooth muscle studied in intact dogs. *Am J Physiol* 217: 154–160, 1969.
34. **Ratkowsky DA.** *Nonlinear Regression Modeling: A Unified Practical Approach*. New York: Marcel Dekker, 1983.
35. **Safar ME, Bouthier JA, Levenson JA, and Simon AC.** Peripheral large arteries and the response to antihypertensive treatment. *Hypertension* 5: III63–III68, 1983.
36. **Safar ME, Toto-Moukouo JJ, Bouthier JA, Asmar RE, Levenson JA, Simon AC, and London GM.** Arterial dynamics, cardiac hypertrophy, and antihypertensive treatment. *Circulation* 75: I156–I161, 1987.
37. **Simon AC, Levenson J, Bouthier JD, and Safar ME.** Effects of chronic administration of enalapril and propranolol on the

large arteries in essential hypertension. *J Cardiovasc Pharmacol* 7: 856–861, 1985.
38. **Simon AC, Levenson J, Chau NP, and Pithois-Merli I.** Role of arterial compliance in the physiopharmacological approach to human hypertension. *J Cardiovasc Pharmacol* 19, *Suppl* 5: S11–S20, 1992.
39. **Simon AC, O'Rourke MF, and Levenson J.** Arterial distensibility and its effect on wave reflection and cardiac loading in cardiovascular disease. *Coron Artery Dis* 2: 1111–1120, 1991.
40. **Stefanadis C, Dernellis J, Vlachopoulos C, Tsioufis C, Tsiamis E, Toutouzas K, Pitsavos C, and Toutouzas P.** Aortic function in arterial hypertension determined by pressure-diameter relation: effects of diltiazem. *Circulation* 96: 1853–1858, 1997.
41. **Stefanadis C, Stratos C, Boudoulas H, Vlachopoulos C, Kallikazaros I, and Toutouzas P.** Distensibility of the ascending aorta in coronary artery disease and changes after nifedipine administration. *Chest* 105: 1017–1023, 1994.
42. **Stefanadis C, Stratos C, Vlachopoulos C, Marakas S, Boudoulas H, Kallikazaros I, Tsiamis E, Toutouzas K, Sioros L, and Toutouzas P.** Pressure-diameter relation of the human aorta: a new method of determination by the application of a special ultrasonic dimension catheter. *Circulation* 92: 2210–2219, 1995.
43. **Stone DN and Dujardin JPL.** Changes in smooth muscle tone influence characteristic impedance of the aorta. *Am J Physiol Heart Circ Physiol* 246: H1–H7, 1984.
44. **Ting CT, Brin KP, Lin SJ, Wang SP, Chang MS, Chiang BN, and Yin FCP.** Arterial hemodynamics in human hypertension. *J Clin Invest* 78: 1462–1471, 1986.
45. **Ting CT, Chen JW, Chang MS, and Yin FCP.** Arterial hemodynamics in human hypertension. Effects of the calcium channel antagonist nifedipine. *Hypertension* 25: 1326–1332, 1995.
46. **Waggoner AD, Barzilai B, Miller JG, and Perez JE.** On-line assessment of left atrial area and function by echocardiographic automatic boundary detection. *Circulation* 88: 1142–1149, 1993.
47. **Watkins RW, Sybertz EJ, Pula K, and Antonellis A.** Comparative effects of verapamil, diltiazem and nifedipine on aortic compliance in anesthetized dogs. *Arch Int Pharmacodyn Ther* 293: 134–142, 1988.
48. **Wolinsky H and Glagov S.** Structural basis for the static mechanical properties of the aortic media. *Circ Res* 14: 400–413, 1964.
49. **Yano M, Kumada T, Matsuzaki M, Kohno M, Hiro T, Kohtoku S, Miura T, Katayama K, Ozaki M, and Kusukawa R.** Effect of diltiazem on aortic pressure-diameter relationship in dogs. *Am J Physiol Heart Circ Physiol* 256: H1580–H1587, 1989.